

STRUCTURE OF PLASMA FORMATIONS AT THE SURFACE OF A CYLINDER IN A  
STREAM OF PARTIALLY IONIZED GAS

V. A. Shuvalov

UDC 533.95:538.4:537.523:550.388.2

In streams of partially ionized gas at the surfaces of bodies there often develop plasma formations having charged particle densities differing from the values of the latter in the undisturbed medium. The presence of such formations alters the functional characteristics of various systems. The investigation of the conditions of formation and the structure of the disturbed zone in the presence of plasma formations is important for an understanding of features of the interaction of bodies with streams of rarefied, partially ionized gas.

The system of equations describing the behavior of the plasma in the disturbed zone near a body in a stream of partially ionized, low-density gas is Vlasov's system of kinetic equations and self-consistent field equations with boundary conditions assigned in the undisturbed medium and at the surface of the body. Considerable difficulties are associated with the solution of such a system. The problem has been solved numerically under rather rigorous restrictions. Therefore, experimental research acquires importance in the study of the properties of the formation and the structure of the disturbed zone near a body in a rarefied plasma stream.

In this article we present the results of an investigation of the structure of the disturbed zone near the surface of a metal cylinder in a hypersonic stream of partially ionized gas in the presence of plasma formations resulting from the influence of the intrinsic magnetic field, the surface potential of the body, and the injection of neutral gas with its subsequent ionization by electron impact.

1. The experimental research was carried out on a gasdynamic plasma installation in a partially ionized nitrogen stream generated by a plasma gas-discharge accelerator. The plasma stream entered the working chamber, in which the pressure of residual gases was  $\sim(1-1.3) \cdot 10^{-4}$  Pa. The parameters of the plasma at the pressure of  $\sim 2 \cdot 10^{-3}$  Pa in the working chamber were measured using three types of movable electrostatic probes — a single cylindrical probe, a plane probe with a working surface 3.5 mm in diameter, made of molybdenum, and a cylindrical probe made in the form of a thermoanemometer [1] with a working part made of tungsten filament 0.06 mm in diameter and 6.5 mm long — and a multielectrode analyzer probe. The single cylindrical probe was made of molybdenum filament 0.09 mm in diameter and 4.0 mm long.

The probe characteristics and the derivatives of the probe current were measured in the automatic mode with two-coordinate recording. The scheme of probe measurements with recordings of the volt-ampere characteristic curves on a recording, direct-current milliammeter, operating in combination with a photomultiplier, using a resistance box as the measurement resistance, allows one to record probe currents in the range of  $1 \cdot 10^{-7}$ – $1.5 \cdot 10^{-1}$  A with smooth regulation of the probe potential from 0 to 250 V. The error in measuring an individual volt-ampere characteristic curve does not exceed  $\pm 2\%$ . The method of harmonics [2] was used to measure voltage derivatives of the probe current. A block diagram of the system for measuring probe-current derivatives is presented in [3]. Since the probe-current derivatives were used only to determine the plasma potential  $\phi_0$ , the amplitudes of the harmonics of the probe current were not calibrated.

Special attention was paid to the surface cleanness of the probes in the measurements of the volt-ampere characteristic curves. Immediately before making the measurements, the working surfaces of the probes were bombarded with a plasma stream and subjected to forced heating to  $\sim 1500^\circ\text{K}$ . The ion branch of the characteristic curve was taken starting with  $\sim 250$  V. The working surfaces of the probes were cleaned by intense bombardment with an ion beam. This makes it possible to eliminate the influence of surface contamination on the results of the probe measurements.

Directional motion did not distort the shape of the probe characteristic curve. The plasma potential was determined by the second-derivative method, as well as from the electron part of the probe characteristic curve, plotted on a semilog scale. The scheme for measuring probe-current derivatives also allows one to record plasma noise in the probe circuit during an experiment, making it possible to monitor the accuracy in measuring the plasma potential  $\Phi_0$ . The maximum plasma noise corresponds to the space potential. It should be noted that the plasma potential found from the point  $d^2I_e/dV^2 = 0$  and the noise maximum corresponds better to the start of the deviation of the semilog characteristic curve from a straight line than does the point of intersection of the asymptotes. A similar phenomenon was observed when determining the space potential using a cylindrical probe built in the form of a thermoanemometer and working in the thermal-probe regime. The plasma potential was determined from the point of divergence of the characteristic curves of the cool and heated probes. The scatter of the measured values of the plasma potential does not exceed  $\pm 4\%$ .

The volt-ampere characteristic curves  $\log I_e = f(V)$  had a clearly expressed straight section. This allowed us to determine the electron temperature in the usual way.

To determine the charged-particle density we used the electron branch of the volt-ampere characteristic curve of the cylindrical probe oriented perpendicular to the stream:

$$N_e = 2\sqrt{\pi}I_{0e}/[Ae(2kT_e/m_e)^{0.5}]; \quad (1.1)$$

$$N_e = [(em_eV)^{0.5}/1.4e^2al](dI_e/dV); \quad (1.2)$$

$$N_e = I_e/[ale(8eV/m_e)^{0.5}]. \quad (1.3)$$

Here  $A$  is the area of the working surface of the probe;  $a$  is the radius;  $l$  is the length of the probe;  $I_{0e}$  is the current to the probe at the plasma potential ( $V = \varphi - \varphi_0 = 0$ ).

A comparison of results on the determination of the charged-particle density in a rarefied plasma stream shows that the use of Eqs. (1.1)-(1.3) for different sections of the electron branch of the volt-ampere characteristic curve of the cylindrical probe yields a scatter of local values of the charged-particle density within the limits of a band characterized by a factor of three [4, 5]. At the basis of such a scatter lies the uncertainty in the choice of the quantity  $I_e$ , corresponding to the plasma potential, as well as the difference between the real probe characteristic curve and the ideal one owing to the effects of secondary emission, electron reflection, etc. Therefore, to increase the accuracy in determining  $N_e$ , the method of uhf diagnostics using an interferometer with a 3-cm range was used in parallel with the probe. The scheme of the uhf interferometer is presented in [6]. The results of determining  $N_e$ , calculated for  $I_e$  measured with plane and cylindrical probes at the point of the upper asymptote of the characteristic curve  $\log I_e = f(V)$  corresponding to the values  $\varphi = \varphi_0$ , found for  $d^2I_e/dV^2 = 0$ , agree satisfactorily with the results of diagnostics [6]. This allowed us to estimate, under the assumption of plasma quasineutrality ( $N_e \approx N_i$ ), the mass stream velocity  $U_\infty$  from the ion branch of the volt-ampere characteristic curve of the plane probe. Since in a plasma jet the velocity scatter of ions is low compared with the velocity of their directional motion, the ion part of the volt-ampere characteristic curve of a plane probe oriented perpendicular to the stream has linearly expressed saturation:

$$I_i = AeN_iU_\infty. \quad (1.4)$$

The energy of the stream ions was determined from the value of the local plasma potential relative to the anode of the source. The resulting values of the ion energy are in satisfactory agreement with the values found using a multielectrode analyzer probe and from the characteristic curve of the plane probe. The scatter of the resulting values of the ion energy of the stream does not exceed  $\pm 4.5\%$ .

The single cylindrical probe used in measurements of the parameters of a plasma stream can undergo rotation about the horizontal and vertical axes of from  $0$  to  $212^\circ$ . The vertical and horizontal rotation are required to obtain the absolute maximum of the ion current. The ratio  $(j_i/j_i^{\infty})_{\max}$  for  $\theta = 0$ , where  $j_i^{\infty} \approx 2alN_iU_\infty(\sin^2\theta - 2eV/MU_\infty^2)^{0.5}$ , was used, in accordance with the theory of the end effect for a cylindrical probe [7], to determine the ion temperature of the stream [8]. It was found that the ion temperature  $T_i$ , like the electron temperature  $T_e \approx 3.5-4$  eV, is practically constant in the working part of the stream,  $T_e/E_1 \approx 4-7$ .

2. The investigations of the structure of the disturbed zone near a cylinder of radius  $R = 3.1$  cm and length  $L = 21$  cm, oriented perpendicular to the velocity vector of the oncoming stream, were made in the working part of a jet with the minimum gradients of the parameters in the axial direction (Fig. 2 of [9]). The cylinder was set up in a cross section of the jet with uniform distributions of the parameters: strength of the external magnetic field  $H = 2$  Oe, i.e.,  $R/\rho_i \approx 1 \cdot 10^{-3}$ ,  $R/\rho_e \approx 1.0$  ( $\rho_\alpha$  is the Larmor radius for particles of type  $\alpha$ ),

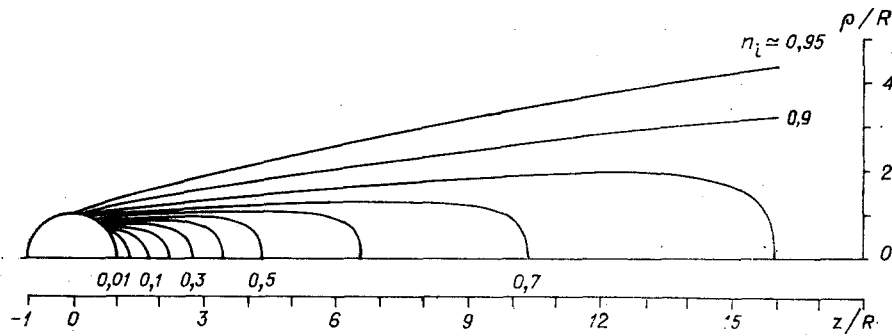


Fig. 1

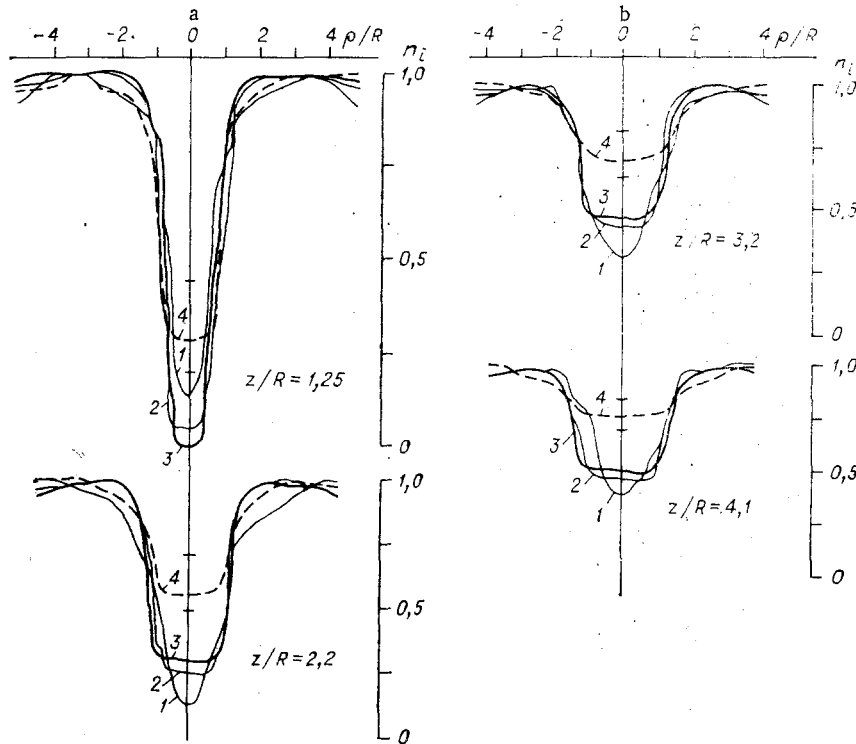


Fig. 2

mass velocity  $U_\infty \approx 21$  km/sec, charged-particle density  $N_\infty \approx 3.7 \cdot 10^9$  cm $^{-3}$ . A device containing a working plasma-generating substance of the type of [10] was set in the body of the metal cylinder. There was a drain element (a cylindrical segment with a central angle of  $\sim 20^\circ$  and a length of 30 mm), insulated from the model, on the surface of the body.

Figure 1 illustrates the structure of the plasma formation resulting from the regime of flow of a supersonic stream of partially ionized gas over a cylinder (a wake) for  $U_\infty / \sqrt{2kT_e/M} \approx 4.3$ ,  $R/\lambda_d \approx 126$ ,  $\phi_s = e\phi_s/kT_e \approx -1.1$ , and  $\phi_s = \phi_{de} \approx e\phi_{de}/kT_e$  ( $\phi_s$  is the potential of the body,  $\phi_{de}$  is the potential of the drain element of the surface relative to the plasma potential, and  $\lambda_d$  is the Debye radius in the working cross section of the jet). The distributions of the normalized  $n_i = I_i(\text{wake})/I_i^\infty$  ion densities were obtained by measuring the current to the plane probe in different cross sections over the length of the wake at a fixed potential corresponding to the region of saturation of the ion branch of the volt-ampere characteristic curve. Here  $I_i(\text{wake})/I_i^\infty$  is the ratio of the disturbed ion current to its undisturbed value in the same cross section  $z/R = \text{const}$ ;  $z$  denotes the distance from the center of the model in the direction of the stream;  $\rho$  is the distance from the center of the model in the transverse direction;  $R$  is the radius of the model. Since the stream velocity  $U_\infty$  is practically constant in the wake, the ion current at a fixed potential is proportional to the ion density [Eq. (1.4)].

The method of creating artificial plasma formations through the injection of a neutral gas with its subsequent ionization by electron impact [10] presumes the presence of positively

charged drain elements on the surface of the body. To estimate the influence of the structural difference between the cylinder used, with an insulated element on the surface, and a smooth metal cylinder, and to distinguish the contributions of each of the factors (the surface potential and the injection of the neutral gas), we investigated the structure of the wake behind the body at different potentials on the surface of the cylinder. The influence of the potential of the cylinder surface on the character of the charged-particle density distribution in the near wake is shown in Fig. 2. Typical families of radial profiles of the normalized ion density, measured with a plane probe, at different distances downstream are presented here. Curve 1 corresponds to a positive potential of the cylinder surface,  $\phi_s = \phi_{de} \approx +9.7$ . Curve 2 pertains to the case when the drain element faces upstream and is at the positive potential  $\phi_{de} \approx +9.7$ , while the rest of the cylinder surface has the negative potential  $\phi_s \approx -1.1$ . Curve 3 denotes the profiles of normalized ion density in the wake behind the cylinder when the drain element has the potential  $\phi_{de} \approx +9.7$ , while the rest of the model surface has  $\phi_s \approx -10.1$ . In this case the ion-density profiles hardly differed from the latter in the wake behind a cylinder, the entire surface of which had the negative potential  $\phi_s = \phi_{de} \approx -10.3$ . A comparison of the values of the charged-particle density for different variants of the potential distribution over the surface (Figs. 1 and 2) indicates the weak influence of the potential of the drain element oriented upstream on the structure of the wake behind the body if the surface area of the cylinder considerably exceeds the surface area of the drain element. The particle distribution in the wake behind a cylinder with a drain element on the surface at  $\phi_s = \phi_{de}$  agrees, to within the error due to the scatter of the stream parameters and the conditions of streamline flow, with the results of measurements of  $n_i$  in the wake behind a smooth cylinder with a uniform metal surface (see Fig. 3 of [11]). Irregularity of the cylinder surface for  $\phi_s = \phi_{de}$  hardly affects the character of the particle distribution in the wake behind the body.

3. The procedure of [10] was used to create artificial plasma formations at the surface of the cylinder. In Fig. 3 we show the structure of the plasma formation (top view) obtained with  $\phi_{de} \approx +9.3$  and the rest of the cylinder surface at the "floating" potential  $\phi_s = -8.1$ , when the drain electrode was oriented toward the oncoming stream. The charged-particle density was determined from the electron branch of the volt-ampere characteristic curve of a cylindrical probe oriented perpendicular to the stream velocity vector ( $n_0 = N_e$ ). The appearance of a plasma formation on the front surface of the cylinder modified the radial profiles of normalized charged-particle density at different distances in the wake (dashed line 4, Fig. 2). The wake fills with slow ions formed by ionization of vapor of the working substance and charge exchange with ions of the stream in the plasma formation. In this case the pressure in the working chamber grew to  $\sim 4.4 \cdot 10^{-3}$  Pa. The charged-particle density distribution (lines of equal density) in the horizontal plane of flow, measured with a cylindrical probe built in the form of a thermoanemometer, is shown in Fig. 4, where  $n_i \approx (N_e \approx N_i) / N_i^\infty$ . According to the results of the probe measurements in the plasma formation on the front surface of the cylinder, two groups of electrons were present: one with a temperature equal to the electron temperature in the oncoming steam and the other with a temperature  $T_e \approx 2$  eV. This is evidently the electron group arising as a result of ionization of vapor of the working substance (polymerized epoxy resin in the present case). The size and structure of the plasma formation and the density level of charged particles in the wake behind the cylinder changed considerably with variation of the potential of the drain electrode. As the potential of the drain electrode was varied from  $\phi_{de} \approx +6$  to  $\phi_{de} \approx +28$  the maximum value of the charged-particle density in the plasma cloud varied from  $10^{10}$  to  $10^{12}$  cm $^{-2}$ . The potential of the rest of the cylinder surface varied in the range of  $-9.8 \leq \phi_s \leq -5.4$ . The corresponding level of variation of the charged-particle density in the wake is denoted by dashed lines in Fig. 2. The structure of the peripheral part of the plasma formations generated on the front surface of the cylinder at different drain-electrode potentials is qualitatively consistent with the density field from a free-molecule source located at the point of the maximum of the normalized charged-particle density [12].

With allowance for the range of variation of  $\phi_{de}$  and  $\phi_s$  with and without plasma clouds present at the surface of the model, the data presented in Figs. 1, 2, and 4 characterize the influence of the injection of neutral gas with its subsequent ionization by electron impact on the structure of the disturbed zone near a metal cylinder in a stream of rarefied, partially ionized gas.

In the course of the experiment the model, located on a positioner, could perform circular rotation about the vertical axis. In this case, for fixed values of the drain-electrode potential and the potential of the rest of the cylinder surface, the structure of the

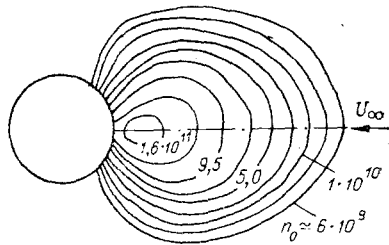


Fig. 3

plasma formation hardly depended on the orientation of the model and the drain electrode relative to the velocity vector of the oncoming stream, even in the case of the injection of vapor of the working substance into the wake behind the body. This made it possible to create a two-sided plasma cloud at the surface on the cylinder. For this the model was equipped with a second device (placed symmetrically to the first) containing the working substance and a drain electrode. Such a construction allowed us to create, at  $\Phi_{de1} \approx \Phi_{de2} \approx +8.6$  and a "floating" potential of the cylinder surface of  $\Phi_S \approx -6.9$ , a plasma formation at the surface of the model with the structure shown in Fig. 5a by injecting neutral gas toward the oncoming stream and into the wake behind the body. In the case where there is a positive potential  $\Phi_{de1} \approx \Phi_{de2} \approx \Phi_S \approx +11.4$  at the surface of the cylinder, an ellipsoidal plasma cloud develops near the model, and with a further increase in the potential of the body it is converted into a nearly coaxial plasma sheath. The structure of the latter is shown in Fig. 5b (top view). The good reproducibility of the structures of plasma formations generated at the surface of the cylinder must be mentioned.

The above data testify to the possibility of varying the charged-particle density distribution in the disturbed zone near a cylinder in a stream of rarefied, partially ionized gas and illustrate the structures of certain plasma formations created through variation of the potential of the body and the injection of neutral gas from the surface.

4. In the second series of tests the device containing the plasma-forming substance was replaced by a solenoid with an outside diameter of 50, an inside diameter of 20, and a height of 34 mm. The influence of its magnetic field on the structure of the disturbed zone near the cylinder in the rarefied plasma stream was investigated. The distribution of the axial and radial-azimuthal components of the solenoid's magnetic field strength, measured by a Hall detector with recording on a two-coordinate plotter with an error of  $\approx \pm 1.5\%$ , is shown in Fig. 6. The intrinsic magnetic field strength of the body is such that a region of locally magnetized plasma develops in the vicinity of the cylinder:  $\rho_e \ll R \ll \rho_i$ . When determining the parameters of such a plasma the plane probe (in the wake) and the cylindrical probe (at the front surface of the body) were oriented perpendicular to the magnetic field strength and stream velocity vectors. The measurements of the charged-particle density were made using the ion branch of the probe characteristic curve. The disturbance of the ion component of the stream was due to the influence of the self-consistent field and illustrates the collective character of the interaction of the plasma stream with the intrinsic magnetic field of the body.

It should be mentioned that with the appearance of a magnetic field, the "floating" negative potential of the body shifts toward positive values, characterized by a decrease

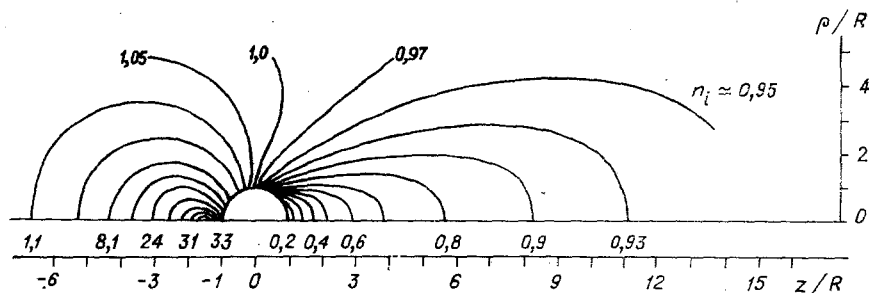


Fig. 4

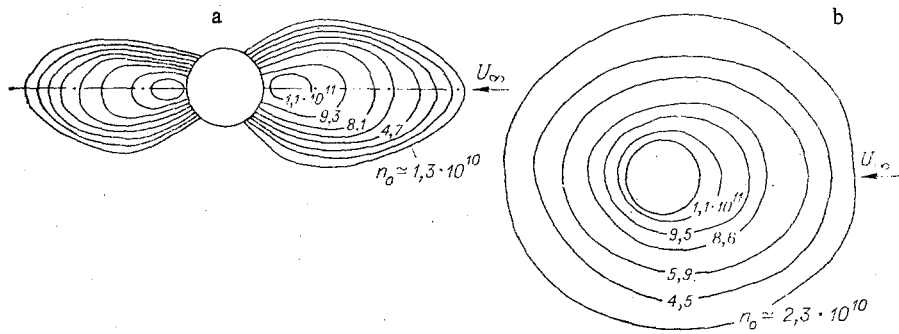


Fig. 5

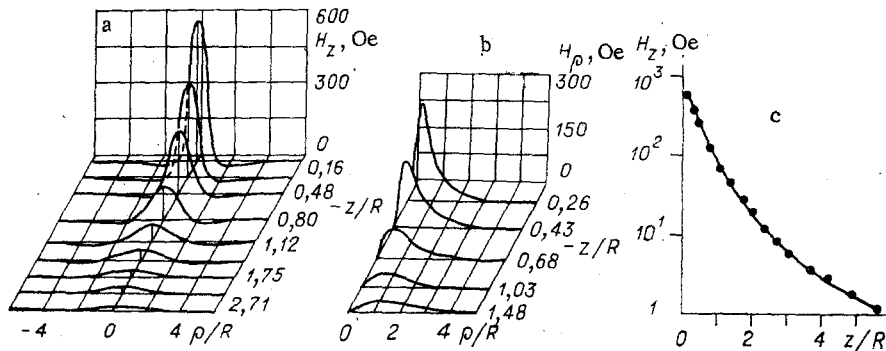


Fig. 6

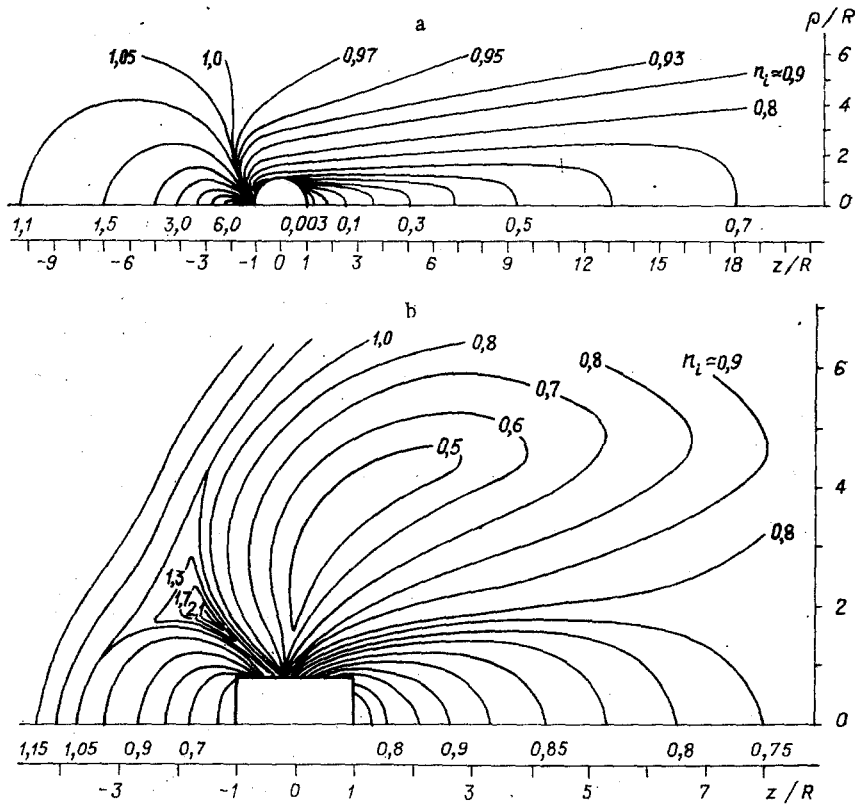


Fig. 7

in the electron flux to the surface of the model. Therefore, it became necessary to hold the potential of the body constant during the measurements.

The structure of the disturbed zone near a transverse cylinder with an intrinsic magnetic field for  $U_\infty/\sqrt{2kT_e/M} \approx 4.3$ ,  $R/\lambda_d \approx 126$ , and  $\Phi_S \approx -1.2$  is presented in Fig. 7a. The

intensity vector of the intrinsic magnetic field of the cylinder is antiparallel to the velocity vector of the oncoming stream. A comparison of the axial values of the charged-particle density with the data of Fig. 1 indicates that the charged-particle density in the wake is considerably reduced with such an orientation of the intrinsic magnetic field; the region of the wake expands. The charged-particle density on the front surface of the cylinder grows with an increase in the magnetic field strength. The character of the variation of charged-particle density in the vicinity of the body with such a magnetic field orientation is qualitatively consistent with the estimates of [13], made for a dipole magnetic field. Here one must keep in mind that the field of a solenoid is a dipole field only at a sufficiently large distance.

The structure of the plasma formations resulting from the influence of an intrinsic magnetic field depends essentially on the orientation of the magnetic field strength vector relative to the velocity vector of the oncoming stream. The structure of the disturbed zone at the surface of a short transverse cylinder of radius  $R = 3.1$  cm and diameter  $L = 5.0$  cm for  $\mathbf{H} \perp \mathbf{U}_\infty$  is shown in Fig. 7b. The strength of the intrinsic magnetic field at the side surface of the model is  $H \approx 90$  Oe. The charged-particle density distribution was obtained for  $U_\infty/\sqrt{2kT_e/M} \approx 4.3$ ,  $\Phi_S \approx -1.8$ ,  $R/\lambda_d \approx 126$ . The structure of the disturbed zone for the case under consideration reflects the main features characterizing the interaction of a supersonic stream of rarefied plasma with a permanent magnetic field for  $\mathbf{H} \perp \mathbf{U}_\infty$ : the presence of cavities at the front and shadow surfaces of the body, the formation of polar cusps, the penetration of charged particles into the wake region, etc. [14, 15].

The results of this research (Figs. 1, 4, and 7 with allowance for the data of Fig. 2) illustrate the influence of the intrinsic magnetic field and the injection of neutral gas from the surface on the character of the flow over a cylinder by a stream of partially ionized gas, and they indicate the possibilities of varying the structure of the disturbed zone near a body in a stream of rarefied plasma.

#### LITERATURE CITED

1. A. M. Khazen and V. A. Shuvalov, "Determination of the parameters of a partially ionized gas with a thermoanemometer," *Zh. Tekh. Fiz.*, 36, No. 2 (1966).
2. O. V. Kozlov, *An Electrical Probe in a Plasma* [in Russian], Atomizdat, Moscow (1969).
3. V. A. Shuvalov, V. V. Gubin, et al., "Plasma parameters of a gas-discharge ion source," *Inzh.-Fiz. Zh.*, 34, No. 1 (1978).
4. V. A. Shuvalov, "Determination of the charged-particle density in a nonequilibrium rarefied plasma from the characteristic curve of a Langmuir probe," *Teplofiz. Vys. Temp.*, 10, No. 3 (1972).
5. C. V. Goodall and B. Polychronopoulos, "Measurement of electron density in low density plasmas from the electron accelerating region characteristics of cylindrical Langmuir probes," *Planet. Space Sci.*, 22, No. 12 (1974).
6. V. A. Shuvalov, A. E. Churilov, and V. V. Turchin, "Diagnostics of a rarefied plasma jet using the probe and uhf methods," *Teplofiz. Vys. Temp.*, 16, No. 1 (1978).
7. J. R. Sanmartin, "End effect in Langmuir probe response under ionospheric satellite conditions," *Phys. Fluids*, 15, No. 6 (1972).
8. V. A. Shuvalov and V. V. Gubin, "Determination of the degree of nonisothermicity of a rarefied plasma stream by probe methods," *Teplofiz. Vys. Temp.*, 16, No. 4 (1978).
9. V. A. Shuvalov, "Structure of the near wake behind a sphere in a nonequilibrium, rarefied plasma stream," *Geomagn. Aeron.*, 19, No. 4 (1979).
10. V. V. Gubin, V. M. Kovtunencko, et al., "Generation of plasma formations at the surface of a body in a partially ionized gas stream," *Teplofiz. Vys. Temp.*, 15, No. 4 (1977).
11. V. A. Shuvalov, "Structure of the near wake behind a cylinder in a nonequilibrium, rarefied plasma stream," *Geomagn. Aeron.*, 20, No. 3 (1980).
12. R. Narasimha, "Collisionless expansion of gases into cavities," *Mekhanika* [collection of translations], No. 2 (1963).
13. Yu. F. Gun'ko and G. V. Loskutova, "Influence of the intrinsic magnetic field on the character of rarefied-plasma flow over a body," in: *Physical Mechanics* [in Russian], Leningr. Univ., Leningrad (1974), Part 1.
14. L. G. Cohen and S. Carlsson, "Experimental investigation of the interaction between a collisionless plasma and an electromagnetic field," *Raket. Tekh. Kosmonavt.*, 7, No. 8 (1969).
15. J. M. Podgorny and E. M. Dubinin, "Laboratory experiments directed toward the investigation on magnetospheric phenomena," *Space Sci. Rev.*, 15, No. 6 (1974).